Unravelling the wind flow over highly complex regions through computational modeling and two-dimensional lidar scanning

Palma, J. M. L. M.; Silva Lopes, A.; Costa Gomes, V. M.; Veiga Rodrigues, C.; Menke, Robert; Vasiljevic, N.; Mann, Jakob

Published in:
Journal of Physics: Conference Series

Link to article, DOI:
10.1088/1742-6596/1222/1/012006

Publication date:
2019

Document Version
Publisher's PDF, also known as Version of record

Unravelling the wind flow over highly complex regions through computational modeling and two-dimensional lidar scanning

IOP Conf. Series: Journal of Physics: Conf. Series **1222** (2019) 012006 doi:10.1088/1742-6596/1222/1/012006

Unravelling the wind flow over highly complex regions through computational modeling and two-dimensional lidar scanning

J.M.L.M. Palma[1], A. Silva Lopes[1], V.M. Costa Gomes[1], C. Veiga Rodrigues[1,3], R. Menke[2], N. Vasiljević[2] and J. Mann[2]

[1] Faculty of Engineering of the University of Porto, Rua Dr. Roberto Frias s/n, 4200-465 Porto, Portugal

[2] DTU Wind Energy, Technical University of Denmark, Frederiksborgvej 399, 4000 Roskilde, Denmark

[3] Currently with Vestas Wind Systems A/S, Design Centre Porto, Rua Lionesa, 4465-671 Leça do Balio, Porto, Portugal

E-mail: jpalma@fe.up.pt, asl@fe.up.pt, vcgomes@fe.up.pt, calvr@vestas.com, rmen@dtu.dk, niva@dtu.dk, jmsq@dtu.dk

Abstract.

Computational modeling and lidar scanning data of the atmospheric flow over a double-ridge (Perdigão) were used to study a 24-hour period on 14–15 May 2017 with a maximum wind speed of more than 6 ms^{-1}. An influence of the stratification was observed throughout most of the time, in the form of a lee-wave triggered by the topography or flow separation further downstream of the ridge. The good agreement between the results obtained by lidar scanning and computational modeling increases our confidence in the use of either of these two techniques. See corresponding video at doi.org/10.11583/DTU.7863482.

1. Introduction

In this study, we show how scanning lidars and three-dimensional time-dependent computational models can be used to increase our knowledge on the flow over complex regions where separated flow, hydraulic jumps and internal gravity waves were observed. These are phenomena that may affect wind power production, but are usually not very well modeled when assessing the wind resources, if modeled at all [1, 2].

Similar phenomena were already observed during Perdigão-2015 [3] and reported in [4], in the case of southwesterly winds. Here we made use of a small set of the Perdigão-2017 field experiment [5, 6] and compared against simplified flow models, both analytical and scale laboratory models [7], with which a good qualitative agreement was found. Quantitative agreement was not sought at this stage, since it is part of an ongoing work, based on a data set larger than the one used here. Our focus is on the flow dynamics of a 24-hour period (starting on May 14 at 18:00 UTC) shown by a video [8], to be found at doi.org/10.11583/DTU.7863482, to which this paper can be considered as a guide.

2. The case study

Perdigão is comprised by two parallel ridges (129.1° and 132.5°, SW and NE ridges), about 1400 m apart and 215 m above the surrounding region, Figure 1. Two field campaigns took place in the region, in 2015 [3] and 2017 [5], with the participation of European and US research groups. The high density of scientific equipment in 2017 has led to a database, still under organization, which is expected to become an important tool for validation and development of computational models.

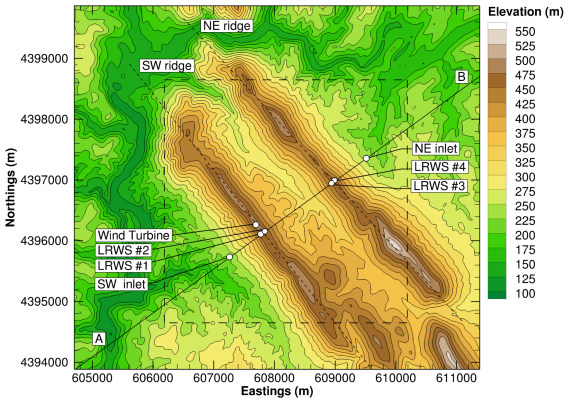

(a) Reference locations (WGS84 UTM 29N): SW and NE ridges and inlet locations, wind turbine and the four long-range wind-scanners (LRWS) along transect A–B (54.7°, relative to the E-W axis). High resolution region, 4 km × 4 km, centred at 4396649N 608198E.

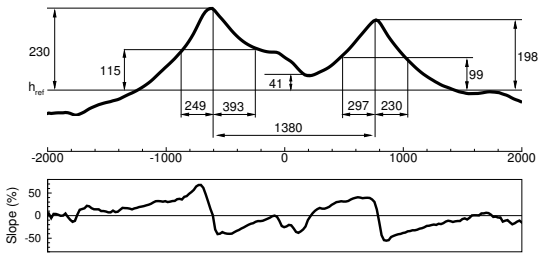

(b) Terrain profile (distance and height in meter, $h_{ref} = 250$ m a.s.l.) and slope along transect A–B.

Figure 1: Perdigão site.

3. Techniques

Computational modeling provides views of the wind flow pattern over large areas, enabling the identification of flow structures beyond the height of meteorological masts. There is no experimental technique other than lidar scanning that can provide similar information.

3.1. Computational modeling

To cover the whole range of scales, a chain of computational models was used, from synoptic with input data from the Global Forecast System [9], passing by WRF [10] mesoscale calculations on three nested domains (37.5, 7.5, and 1.5 km grids), to micro scales resolved by VENTOS®/M [11]. The Reynolds averaged and the $k - \varepsilon$ two-equation turbulence model equations were discretised in a domain of 18 km × 18 km × 10 km; a region (dashed square in Figure 1a) was horizontally resolved by a regular mesh (40 m), 4 m height close to the ground [4]. Conditions at the boundaries were updated every 5 min by the WRF results on the 1.5 km grid. The time step was equal to 1.5 s. The 24 hour (57600 individual time step calculations) animation [8] consists of 288 frames averaged to 5-minute period (200 time steps), running at 5 frames per second.

3.2. Lidar scanning

For this study we deployed measurements from four scanning-Doppler lidars [12] on top of the ridges (LWRS #1 to #4, in Figure 1a). They performed range-height-indicator (RHI) scans along transect A–B (SW–NE direction), covering a distance of up to 3 km on both sides outside

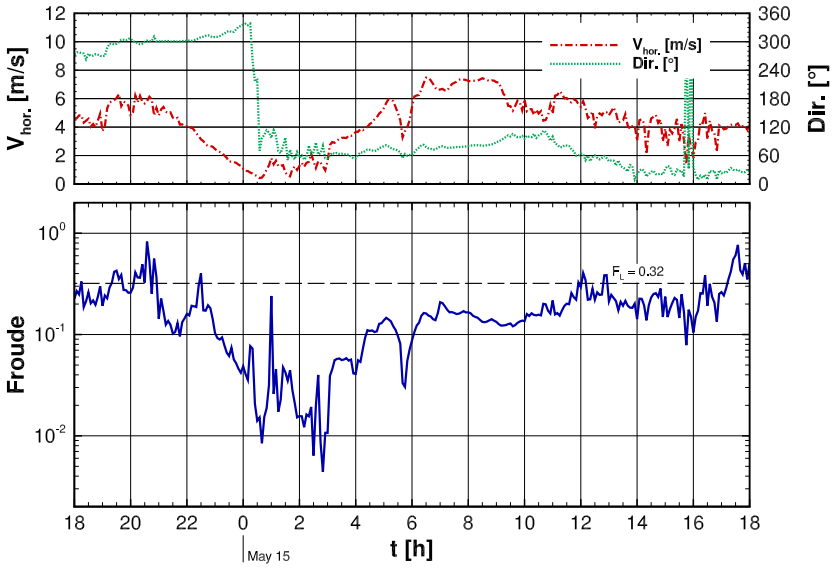

(a) At SW inlet (in Figure 1a), 715 m SW of SW ridge.

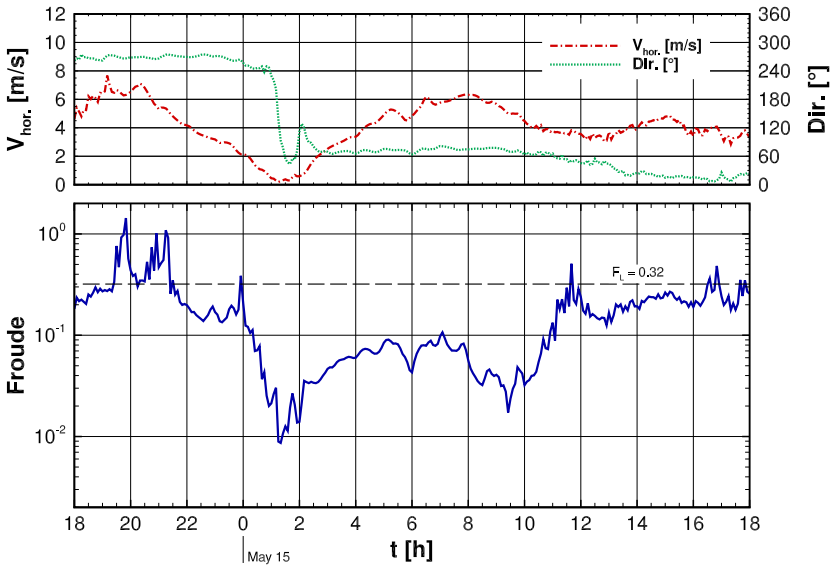

(b) At NE inlet (in Figure 1a), 715 m NE of NE ridge.

Figure 2: Froude number, wind speed and direction at h_{agl} = 215 m agl, from 14 May 18:00 UTC until 15 May 18:00 UTC. $F_L = 0.32$, critical Froude number.

of the valley and the region in between the ridges (Figure 1b). Measurements were taken continuously during the upward movement of the scanning beams, with an averaging elevation speed of 0.75° per second over a range of 3°. Range gates were placed every 15 m up to a distance of 3000 m and starting at a distance of 100 m from the scanners. The probe length (full-width at half maximum) of the scans was about 30 m along the laser light propagation path. Thus measurement volumes overlapped and the effective size of the measurement volumes increased with distance because of averaging in the transverse direction while scanning. A single scan took about 24 seconds to complete. We filtered the data using several consecutively applied methods to remove measurements that are influenced by hard targets and other artefacts. The 24-hour animation consists of 3168 individually acquired scans averaged to 5-minute intervals (11 scan)

and runs at a speed of 5 frames per second.

4. Wind flow conditions: speed, direction and Froude number

Stratification was characterised by the Froude number, $F = U/(Nh_{agl})$, where U is the wind speed at h_{agl} (215 m agl) and N, the Brunt-Väisälä frequency, is equal to $\sqrt{g/\theta\,\partial\theta/\partial z}$, where g is the gravitational acceleration, and θ and $\partial\theta/\partial z$ are the potential temperature and its gradient at the ridge height (h_{agl}).

To monitor the flow development, we show (Figure 2) the computational results of the wind speed and direction, and the Froude number southwest of SW ridge and northeast of NE ridge, from 18:00 (14 May) to 18:00 (15 May). There are two main periods: until and after 00:00. The northwesterly wind (270°), rotates clockwise to NE (60°), remaining almost perpendicular ($\approx 70°$) to the NE ridge (129.1°) until 13:00. The wind rotation, which occurs within a relatively short period of time (30 minutes), is noticed first (one hour earlier, at 00:00) in the south side of the SW ridge (Figure 2a). The rotation, though fast, is accompanied by a wind deceleration from more than 6 ms^{-1} to nearly no wind (less than 1 ms^{-1}), between 00:30 and 03:00, with the Froude number reaching a minimum of 0.003 at 02:45. The nighttime period, as expected, displays the features of a stably stratified atmosphere, with a smoother wind speed time series compared with the spikier shape during the afternoon, typical of an unstable convective boundary layer.

5. Flow patterns

In this section, we present the flow patterns over the double-ridge, based on the longitudinal velocity along transect, streamlines, and potential temperature predicted by the computational model, and the radial velocity measured by the lidars in transect A–B, Figure 1a.

5.1. Phase 1: single layer structure

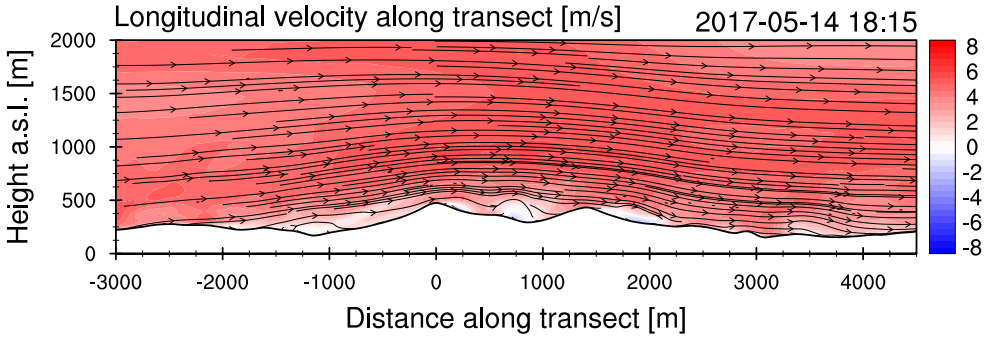

Figure 3: 14 May 2017 18:15 UTC. Streamlines and longitudinal velocity. Computational results are VENTOS®/M micro-scale results (40 m grid) coupled with WRF results (1.5 km grid), based on input data from NCEP; the terrain is plotted in white.

At 18:15 May 14, the westerly ($\approx 270°$, Figure 2a) wind shows in Figure 3 from left to right. Separated flow regions appear on lee-side of both ridges, starting at the top, due to adverse pressure gradient; i.e., the flow displays characteristics of a neutral atmosphere. Based on [7], assuming two-dimensional laminar flow, the critical Froude number $F_L = D/(L\pi)$, below which no waves are possible and flow separation is boundary-layer controlled, is equal to 0.32; here, D, the water tank depth in the laboratory experiment [7], was taken as the free atmosphere height, equal to 1500 m, also equal to L, the width of a single hill in Perdigão. Given the differences between the real flow and the laboratory experiment [7], the agreement between F_L and the

Froude number in Figures 2a and 2b can be considered as a rule of thumb that nevertheless will be used as an indication of nearly unstratified flow between 18:00 and 22:00 May 14.

5.2. Phase 2: the low-level jet from NE and the two-layer structure

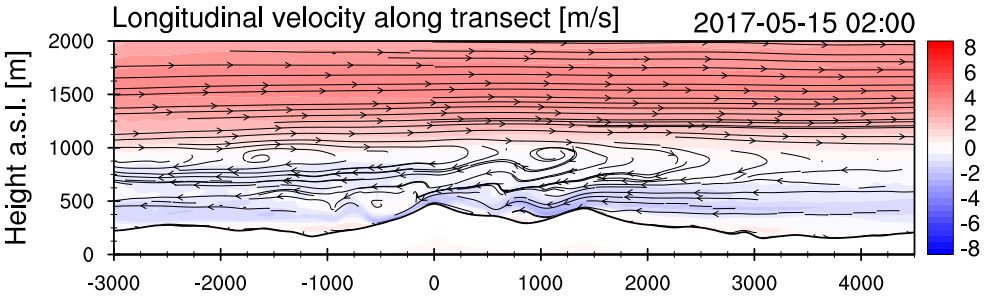

(a) Streamlines and longitudinal velocity. Computations as in Figure 3.

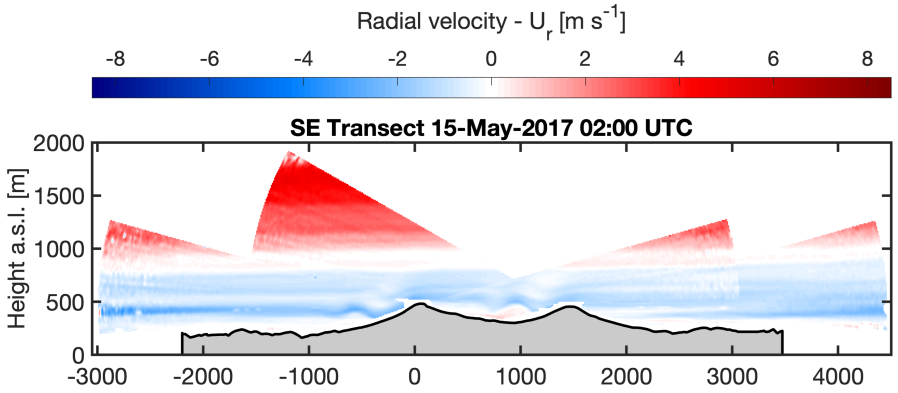

(b) Radial (along the laser beam) velocity, minus sign indicates flow towards the southwest (from right to left in the plot). Scanning lidar results are composite of four range-height-indicator scans; the terrain is plotted in grey.

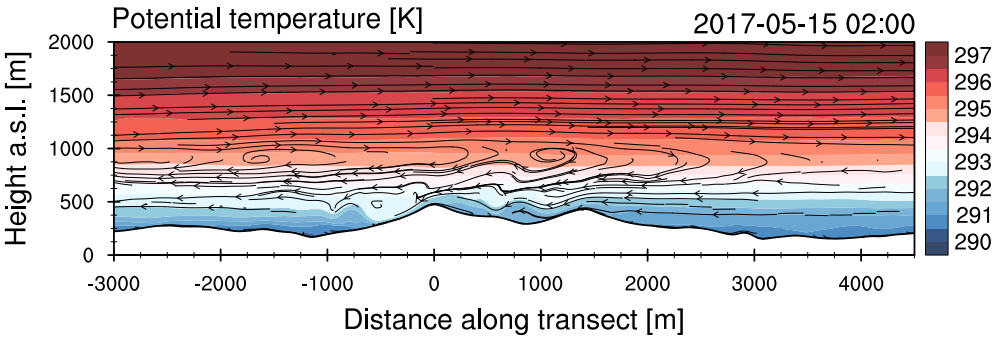

(c) Potential temperature. Computations as in Figure 3.

Figure 4: 15 May 2017 at 02:00 UTC.

During the next four hours (22:00–02:00 UTC), a two-layer structure develops (Figure 4a and 4b): an upper layer (above 1000 m a.s.l.), free atmosphere, made of southeasterly winds, decoupled from the bottom layer (below 800 m) of low wind speed flow, driven by a northeasterly jet flow of cold air at 500 m a.s.l. (Figure 4c). As the jet strength increases, the flow accelerates

over the two-ridge topography, and internal lee-waves emerge. Separated flow regions do not occur on the lee-sides, they are not set by pressure gradient and the Froude number is about 0.03 (Figures 2a and 2b). According to [13] the low-level jet (LLJ) originates from the plateau between Serra da Estrela and Sierra de Gata mountain ranges, N and NE of Perdigão and the turning of the wind direction is induced by slope and valley winds under weak synoptic conditions.

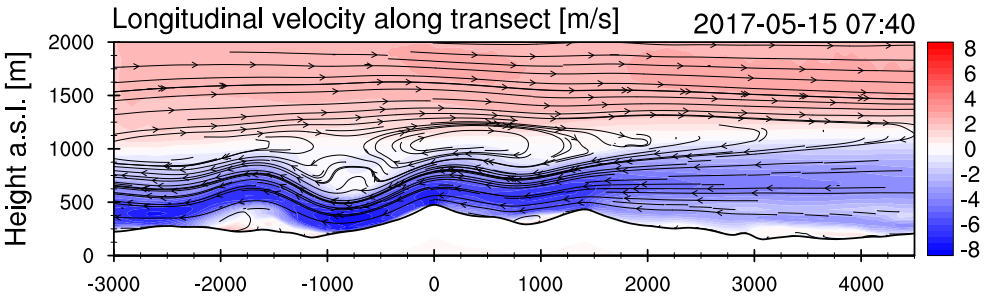

(a) Streamlines and longitudinal velocity. Computations as in Figure 3.

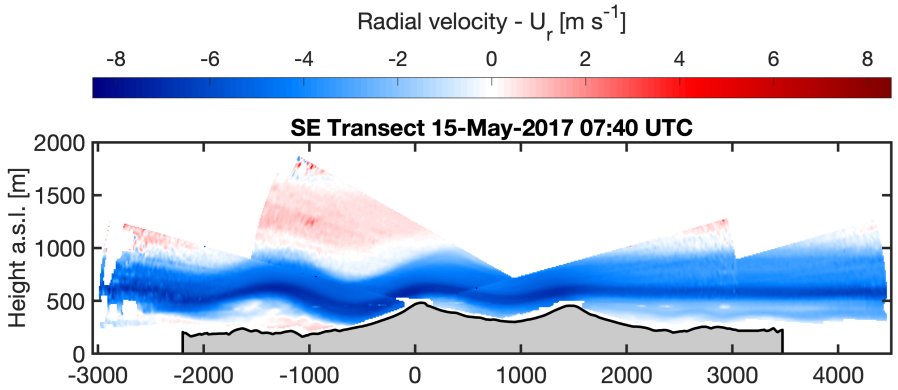

(b) Radial (along the laser beam) velocity, minus sign indicates flow towards the southwest (from right to left in the plot). Scanning lidar results are composite of four range-height-indicator scans; the terrain is plotted in grey.

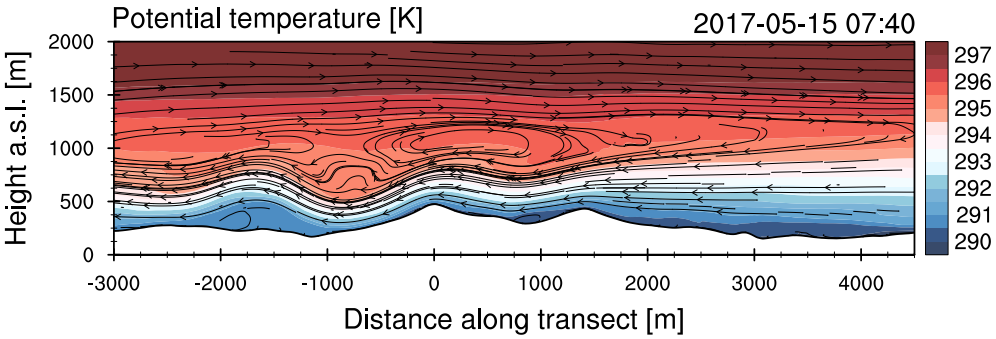

(c) Potential temperature. Computations as in Figure 3.

Figure 5: 15 May 2017 at 07:40 UTC.

The lee-wave pattern is the characteristic of most of the nighttime period, with Froude number about 0.1 (Figures 2a and 2b). Figure 5, at 07:40, was selected among many, by its quality to illustrate the atmospheric phenomena being present during this period and the

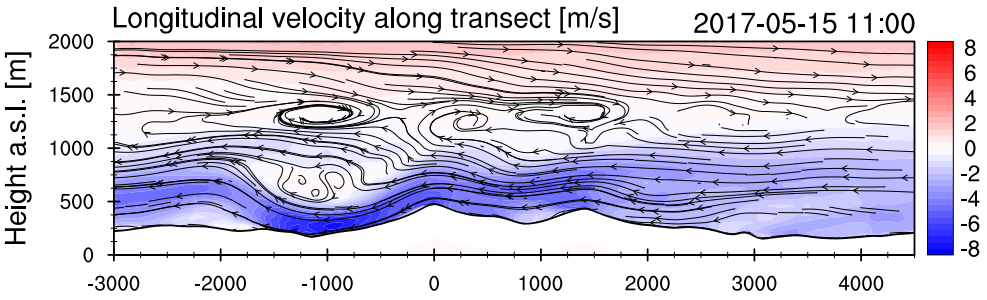

(a) Streamlines and longitudinal velocity. Computations as in Figure 3.

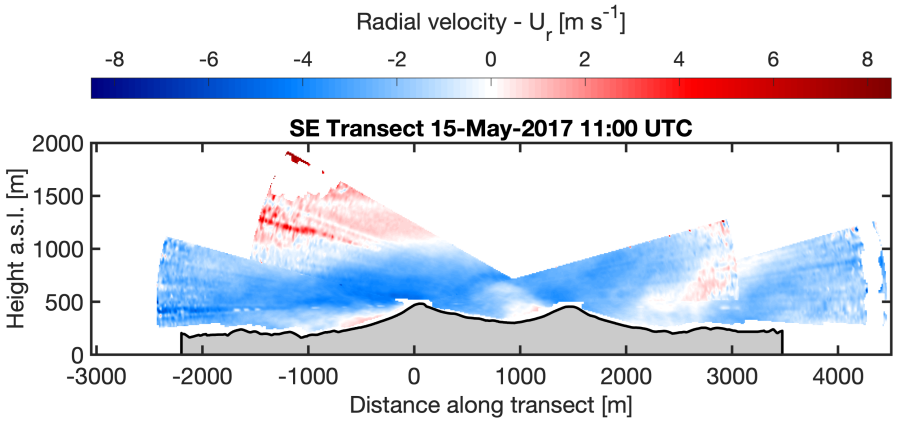

(b) Radial (along the laser beam) velocity, minus sign indicates flow towards the southwest (from right to left in the plot). Scanning lidar results are composite of four range-height-indicator scans; the terrain is plotted in grey.

Figure 6: 15 May 2017 at 11:00 UTC.

ability of both the remote sensing and the computational techniques to capture them. The lee-waves, triggered by the first (NE) ridge, have a wavelength of about the distance between ridges ($\lambda \approx 1400$ m, Figure 1b) and reach a height of 1000 m; i.e., they are trapped upwards by the top homogeneous layer of southwesterly winds, with a transition layer in between, made of large and highly stretched (length/height ratio higher than 10) vortex structures. The waves have a major impact on the flow, yielding a high wind speed (6 m/s) at the top of the ridge, at a distance of about 100 m agl, with consequences on the operation of wind turbines. The flow is almost fully attached in the valley. In the lee-side of the second hill there is no wake vortex, as would be expected under neutral conditions; on the other hand, after the hill at $x = -1500$ m and close to the ground, a lee-wave-type rotor [14] was observed and predicted. Both lidar scanning and computational model agree on the time of occurrence, length, height and location of this region, which is also a large mass of cold air, as shown by the potential temperature in Figure 5c. The agreement goes through the whole nighttime, from the beginning until the end of the lee waves, including cycles of creation and destruction of this rotor structure via hydraulic jump. This is also an indication of the sensitivity of the flow pattern to the Froude number variation experienced during the night.

5.3. Phase 3: the convective boundary layer and the end of the two-layer structure

The time of the establishment of an unstable atmosphere is typically 3 to 5 hours after sunrise (at 6:20), as can be seen on the Froude number increase after 10:00 (Figure 2). At 11:00, Figure 6,

both the computer model and the lidar measurements display high activity in the transition layer, about 1000 m, reaching up to 1500 m. The wave-like structure is weakened, after which a new cycle will be reinitialised.

6. Conclusions

The observations by scanning lidars of the Perdigão site showed a large variety of flow phenomena, namely an accelerating low-level jet over two ridges, gravity waves with a length equal to the inter-ridge distance, attached flow downstream of both ridges and a stationary rotor 1500 m downstream of the downwind ridge. All these characteristics were well reproduced by the coupled models.

The good qualitative agreement between the results obtained by scanning lidar and computational modeling increases our confidence in the use of either of these two techniques. Many aspects of the physics of the atmosphere were disclosed that are relevant to wind resource analysis and wind turbine operation, which cannot be revealed by point-based measurements.

As a final note, because Figures 3–6 cannot convey a comprehensive view of the flow, with all its dynamics and complexity, we strongly recommend the viewing of the video [8] corresponding to this study.

Acknowledgments

The Perdigão-2017 field campaign was primarily funded by the US National Science Foundation, European Commission (ENER/FP7/618122/NEWA), Danish Energy Agency, German Federal Ministry of Economy and Energy, FCT-Portuguese Foundation for Science and Technology, (NEWA/1/2014), and US Army Research Laboratory.

We are grateful to the municipality of Vila Velha de Ródão, landowners who authorized installation of scientific equipment in their properties, the residents of Vale do Cobrão, Foz do Cobrão, Alvaiade, Chão das Servas and local businesses who kindly contributed to the success of the campaign. The campaign would not have been possible without the alliance of many persons and entities, too many to be listed here and to whom we are also grateful.

References

[1] G A M van Kuik and *et al*. Long-term research challenges in wind energy – a research agenda by the European Academy of Wind Energy. *Wind Energ. Sci.*, **1**:1–39, doi:10.5194/wes-1-1-2016, 2016.

[2] J M L M Palma, F A Castro, L F Ribeiro, A H Rodrigues, and A P Pinto. Linear and nonlinear models in wind resource assessment and wind turbine micro-siting in complex terrain. *J. Wind Eng. Ind. Aerod.*, **96**:2308–2326, doi.org/10.1016/j.jweia.2008.03.012, 2008.

[3] N Vasiljević, J M L M Palma, N Angelou, J C Matos, R Menke, G Lea, J Mann, M Courtney, L F Ribeiro, and V M M G C Gomes. Perdigão 2015: methodology for atmospheric multi-Doppler lidar experiments. *Atmos. Meas. Tech.*, **10**:3463–3483, doi.org/10.5194/amt-10-3463-2017, 2017.

[4] C V Rodrigues, J M L M Palma, N Vasiljević, M Courtney, and J Mann. Coupled simulations and comparison with multi-lidar measurements of the wind flow over a double-ridge. *J. Phys. Conf. Ser.*, **753**:032025, doi.org/10.1088/1742-6596/753/3/032025, 2016.

[5] H J Fernando and *et al* The Perdigão: peering into microscale details of mountain winds. *Bull. Am. Meteorol. Soc.*. (In press), doi:10.1175/BAMS-D-1-0227.1, 2019

[6] J Mann and *et al*. Complex terrain experiments in the new european wind atlas. *Philos. Trans. Royal Soc. A*, **375**:(2091):20160101, doi.org/10.1098/rsta.2016.0101, 2017.

[7] J C R Hunt and W H Snyder. Experiments on stably and neutraly stratified flow over a model three-dimensional hill. *J. Fluid Mech.*, **96**:671–704, 1980.

[8] R Menke, J M L M Palma, J Mann, N Vasiljević, A S Lopes, V M C Gomes and C V Rodrigues. Animation of lidar and simulation data of complex flow over the Perdigão measurement site, doi.org/10.11583/DTU.7863482, 2019.

[9] Global Forecast System (GFS). https://www.ncdc.noaa.gov/data-access/model-data/model-datasets/global-forcast-system-gfs.

[10] W C Skamarock, J B Klemp, J Dudhia, D O Gill, D M Barker, M G Duda, X -Y Huang, W Wang, and J G Powers. A description of the advanced research WRF version 3. NCAR/TN-475+STR. Technical report, Mesoscale and Microscale Division, NCAR, Boulder, Colorado, USA, 2008.

[11] C V Rodrigues, J M L M Palma, and Á H Rodrigues. Atmospheric flow over a mountainous region by a one-way coupled approach based on Reynolds-averaged turbulence modelling. *Boundary Layer Meteorol.*, **159**:407–437, dx.doi.org/10.1007/s10546-015-0116-7, 2016.

[12] N Vasiljević, G Lea, M Courtney, J-P Cariou, J Mann, and T Mikkelsen. Long-range windscanner system. *Remote Sens.*, **8**(11):896, 2016.

[13] J Wagner, T Gerz, N Wildmann, and K Gramitzky. Long-term simulation of the boundary layer flow over the double-ridge site during the Perdigão 2017 field campaign. *Atmos. Chem. Phys.*, **19**:1129–1146, doi.org/10.5194/acp-19-1129-2019, 2019.

[14] L Strauss, S Serafin, and V Grubišić. Atmospheric rotors and severe turbulence in a long deep valley. *J. Atmos. Sci.*, **73**:1481–1506, doi.org/10.1175/JAS-D-15-0192.1, 2016.